On the optimal sizing of batteries for electric vehicles and the influence of fast charge

Mark W. Verbrugge[1] and Charles W. Wampler
Chemical and Materials Systems Lab
General Motors Research and Development
Warren, MI 48092-2031, USA

Abstract

We provide a brief summary of advanced battery technologies and a framework (i.e., a simple model) for assessing electric-vehicle (EV) architectures and associated costs to the customer. The end result is a qualitative model that can be used to calculate the optimal EV range (which maps back to the battery size and performance), including the influence of fast charge. We are seeing two technological pathways emerging: fast-charge-capable batteries versus batteries with much higher energy densities (and specific energies) but without the capability to fast charge. How do we compare and contrast the two alternatives? This work seeks to shed light on the question. We consider costs associated with the cells, added mass due to the use of larger batteries, and charging, three factors common in such analyses. In addition, we consider a new cost input, namely, the cost of adaption, corresponding to the days a customer would need an alternative form of transportation, as the EV would not have sufficient range on those days.

[1] Corresponding author, mark.w.verbrugge@gm.com

Introduction

We are at a crossroads in terms of balancing two promising technologies: (1) higher energy density (Wh/L) and specific energy (Wh/kg) batteries, relative to today's conventional graphite/metal-oxide lithium ion systems, and (2) fast-charge capability, defined here as greater than Level 2 charging, or greater than about 20 kW. Currently in the United States, conventional Level 2 charging of 6.6 kW is available in homes and various community locations. In the ideal case, high energy batteries would be able to accommodate fast charge, but two of the more promising high-energy cell technologies, Si-enhanced [1-31] and Li-metal negative electrodes [32-45], are problematic in this respect. For Si-enhanced electrodes, the limiting factor is that the lithium diffusion coefficient in Si is about two orders of magnitude lower than in graphite (see, for example, [9]), whereas Li-metal electrodes suffer from dendrite-related shorting of cells at higher rates of charging (see [41-44] and references therein). The tradeoff between high-energy and fast-charge capability poses a dilemma in the design of electric vehicles (EVs).

Herein we derive and implement a simple model to assist in evaluating such matters as cell performance, cost, life, and fast-charge capability. The approach is useful in terms of comparing and contrasting battery systems and shedding light on technological tradeoffs.

A framework for approaching EV design and architecture

Because EVs are usually range-constrained relative to conventional ICEVs, we need to estimate the cost for the customer to adapt to a new mode of transportation when the EV fails to provide the needed driving distance. Pearre et al. [46] have studied this problem and found it expedient to assume that the days of adaptation per year N_A is a function of the vehicle range *x*, and no other variables. We employ the 75 percentile driver[2] data of [46]. To facilitate computations, we fit $N_A(x)$ with a cubic spline function, as detailed in the Appendix and plotted in Figure 1.

[2] The 75 percentile driver requires adaption $N_A(x)$ days per year; on all other days of the year, the driver's needs are satisfied by the EV range *x*.

For our cost function *S*, we consider four components, S_{cell}, S_{chg}, S_A, and S_M, corresponding to cell, charging, adaptation, and added-mass costs, respectively:

1) $$S = S_{cell} + S_{chg} + S_A + S_M$$

The variables and parameters used in this work, and base values, where appropriate, are provided in Table 1. Given an EV range *x* based on a single (full) charge of a battery pack with useable capacity *Q*, we can immediately calculate cell and added-mass costs: $S_{cell} = Qs_{cell} = Cxs_{cell}$ and $S_M = \left((Cx / q_{SE}) - M_0\right)s_M$, respectively, where *C* is the energy consumption per unit distance for the vehicle and M_0 is the reference mass as described in Table 1.

We shall consider two forms of EVs in terms of charging capability: those that use a conventional, Level 2, 220 V charger of 6.6 kWh and those for which a fraction *f* of the pack capacity *Q* can be fast charged in time τ. The cost for charging the vehicle over its lifetime *t*, in the absence of fast-charge capability, is given by $S_{chg} = \left(365 - N_A\right)m_{avg}tCs_{chg}$, where $365 - N_A$ corresponds to the days per year the EV is charged. For fast-charge EVs, the range of the fully charged battery, *x*, plus that of one fast charge is thus $(1+f)x$. We do not consider more than one fast-charge event, as it is less likely that the customer will want to use the EV to drive distances longer than $(1+f)x$ by successively fast charging; that is, we assume that the customer would adapt to an alternative form of transportation if her/his trip were projected to exceed the range $(1+f)x$, and the days of adaptation/year with fast charge is N_A evaluated at $(1+f)x$, or $N_A\left((1+f)x\right)$. In addition, because we assume that the number of fast-charge events would be small and can be neglected in the charging cost, we estimate the lifetime charging cost based on the average daily mileage m_{avg} as:

2) $$S_{chg} = \left[365 - N_A\left((1+f)x\right)\right]m_{avg}tCs_{chg}$$

Because fast charge capability increases the number of days the EV is driven, i.e., because $N_A\left((1+f)x\right) < N_A(x)$, the charging cost increases with fast charging, but for the same reason, the adaption cost with fast charging, $S_A = N_A\left((1+f)x\right)ts_A$, decreases from that of conventional

Level 2 charging, corresponding to $f = 0$. Last, it is important to understand the power P_{FC} needed for fast charge:

3) $$P_{FC} = \frac{fQ}{\tau} = \frac{fC}{\tau} x$$

In summary, the total cost function with fast charging is given by

4) $$S(x) = \underbrace{Cxs_{cell}}_{S_{cell}(x)} + \underbrace{\left[365 - N_A\left(x(1+f)\right)\right] m_{avg} t C s_{chg}}_{S_{chg}(x)} + \underbrace{N_A\left(x(1+f)\right) t s_A}_{S_A(x)} + \underbrace{\left(\frac{Cx}{q_{SE}} - M_0\right) s_M}_{S_M(x)}$$

We can identify the optimal range with respect to our total cost function by solving for x when $dS/dx = 0$:

5) $$\frac{dS}{dx} = Cs_{cell} + \frac{d}{dx}\left[N_A\left((1+f)x\right)\right]\left(-m_{avg} C s_{chg} + s_A\right) t + \frac{C}{q_{SE}} s_M = 0$$

This equation can be solved for the optimum range x for which the cost function is minimized. (As discussed in the Appendix, when N_A is a cubic spline, dS/dx is piecewise quadratic, so the optimality condition 5 can be solved analytically.)

Results and discussion

Plotted in Figure 2 are three cases. As noted in Table 1, we examine a conventional cell technology (e.g., similar to that of the Chevrolet Bolt EV), the same cell with fast-charge capability (f = 80% of the cell capacity charged in τ = 15 minutes), and a high-energy cell corresponding to the USABC 2020 goals, but no fast-charge capability. The only cost component that decreases with range is the adaptation cost. Hence, if the cost of adaptation is ignored, no minimum in the cost function results, and an optimal range cannot be determined. For the parameters chosen, the best value for the customer is the fast-charge scenario (middle plot, 52.3 L of cells and an optimal total range of $(1 + f)x$ = 203 miles, which includes one fast charge at a charge rate of 90 kW). For all three plots of Figure 2, the optimal total range and cost are marked by a triangular symbol and numerical values are provided. Because we employ a Bolt-like vehicle, upon completing the calculation associated with Eq. 5, which employs the

consumption value C = 250 Wh/mile of Table 1, we must check to ensure that the volume of cells is less than or equal to that of a Bolt-like EV (113 liters). The volume of cells is given by

6) $$V_{cell} = \frac{Cx}{q_{ED}}$$

No credit is taken in the calculation for the cell volumes being less than 113 L. For the fast-charge analysis, even at 400 miles total, the net cell volume of 105 L is below the 113 L allocation. For the uppermost and lowermost plots, a symbol is used to indicate the range (and cost) when 113 L of cells are employed; higher ranges are not of practical importance insofar as the cells would not fit in a Bolt-like EV without taking away interior volume from the customer or adding exterior volume, which would alter the vehicle energy consumption parameter C.

Sensitivities to the specific costs and the fast-charge fraction are displayed in Figure 3; the abscissa is the indicated parameter divided by its base value specified in Table 1. Thus, the ranges analyzed include

s_A	27.5 to 82.5 \$/day (curve labeled s_A, with a base value of 55 \$/day) 55 to 165 \$/day (curve labeled $2s_A$)
s_{cell}	75 to 225 \$/kWh for the 250 Wh/kg, 530 Wh/L battery with a base value of 150 \$/kWh 50 to 150 \$/kWh for the 350 Wh/kg, 750 Wh/L battery with a base value of 100 \$/kWh
s_M	5 to 15 \$/kg with a base value of 10 \$/kg
f	0.4 to 1 (fraction of the pack that can be fast-charged in time τ), with 100 and 150 \$/kWh cell costs for the 250 Wh/kg, 530 Wh/L battery and 100 \$/kWh for the 350 Wh/kg, 750 Wh/L battery, respectively, with the base value of 0.8

For each curve in Figure 3, the parameter in question begins at the left abscissa value, at 0.5 times its base value, and the labeled parameter increases linearly with the abscissa value until it reaches 1.5 times it base value. All other parameters are held constant and equal to their base value unless otherwise indicated. For all curves, f = 0 unless it is specified. The results of Figure 3 indicate that a greater EV range is optimal for higher adaptation costs, lower cell costs, and lower costs for added mass. Improved fast-charge capability (larger f) leads to lower vehicle range for the fully charged pack (lower dashed lines of the plots), but larger total range when one additional fast-charge is included (upper solid lines). The curve labeled $1.95s_A$ bears similarity to the Chevrolet Bolt EV in terms of pack size and range. All curves associated with fast charging

end at an abscissa value of 1.25/0.8 = 1, or 100% of the battery pack can be fast charged. The maximum cell volumes are called out in Figure 3; all cell volumes are below 113 L for the calculations depicted. For much lower cell costs or higher adaptation costs, the volume limit would be exceeded, which would then limit the battery pack size and energy.

Using the optimal ranges displayed in Figure 3, the cost function of Eq. 4 can be evaluated, and commensurate results are presented in Figure 4. Steeper slopes in the curves are indicative of a greater impact on the cost function for changes in the associated parameter. We see that the cost function is more sensitive to the cell and adaptation costs and less sensitive to the added-mass cost.

Summary and conclusions

A framework is described that allows one to calculate the optimal range for an EV, including the influence of fast charging. Because of the real-world complexity of the problem, the presented results must be viewed as qualitative, but the approach does identify key factors that should be considered in battery sizing. (The time value of money is not considered in the model.)

Of particular note is the cost of adaptation. When we exercise the model with inputs one can associate with a battery like that of the Chevrolet Bolt EV, we find that the net cell volume and the vehicle range are consistent with an adaptation cost of $165/day, three times the average cost per day to rent a car in the United States. This adaptation cost would be appropriate for customers having a strong desire to avoid relying on some alternative method of transportation for the days in which the EV could not supply the needed miles. (Per Figure 1, the Bolt EV's 238 miles range would mean that drivers would need an alternative form of transportation—that is, they would need to adapt—about 5 days per year.)

The results of Figure 2 allow one to assess whether fast-charge of a conventional lithium ion battery is superior to the implementation of a high-energy density cell that cannot be fast charged. For the parameters chosen, fast-charge of a conventional lithium ion battery offers superior value to the customer relative to the high-energy density cell. Sensitivity of the model to parameter values are the subject of Figure 3 and Figure 4.

Our approach of using the cost of adaptation days to determine the optimum range is new; we acknowledge, however, that the actual adaptation cost will vary across the pool of potential EV buyers.

Many customers can be expected to own an ICEV (a vehicle with an internal combustion engine) as well as an EV, so the adaptation cost would be minimal. Regional influences (e.g., a city versus a rural location) would be important. Shared-use mobility solutions also offer lower cost adaptation, but they are not identical in customer value with personal transportation. More generally, as noted above, while the framework presented in this analysis identifies key factors to consider in EV architectural design, battery sizing, and the value of fast charging, many open questions remain in terms of quantifying key parameter values. As more demographic data on driver needs becomes available, refinements to the model might include a Monte Carlo approach with probability distributions for various quantities.

Appendix

For the piecewise spline, three intervals are used; the intervals and the spline coefficients for each interval are provided in the following table.

Range (miles)	Interval j	a_j	b_j	c_j	d_j
100 to 150	1	8.6452	-76.3887	242.1196	-263.1208
150 to 325	2	1.6775	-6.7117	9.8629	-5.0579
325 to 500	3	0.209	0.066	-0.5643	0.2894

The cubic splines for each interval j can be used to represent the adaptation days:

$$\frac{N_A}{25} = a_j\left[\frac{x(1+f)}{500}\right]^3 + b_j\left[\frac{x(1+f)}{500}\right]^2 + c_j\left[\frac{x(1+f)}{500}\right] + d_j$$

which is plotted along with the data in Figure 1 (with $f = 0$). The constants 25 and 500 have units of days and miles, respectively. The curve in Figure 1 is the least-squares fit of a cubic spline to the indicated data points for a choice of break points at 150 and 325 miles, subject to the constraint that the first derivative be monotonic, or equivalently, that the second derivative be always positive. A description of how to construct cubic splines and their utility can be found in [47].

Using the derivative

$$\frac{dN_A}{dx} = \tilde{a}_j x^2 + \tilde{b}_j x + \tilde{c}_j$$

where

$$\tilde{a}_j = 3(25)\left(\frac{1+f}{500}\right)^3 a_j,\ \tilde{b}_j = 2(25)\left(\frac{1+f}{500}\right)^2 b_j,\ \tilde{c}_j = 25\left(\frac{1+f}{500}\right)c_j$$

and Eq. 5, we can write

$$\frac{dN_A}{dx} = \tilde{a}_j x^2 + \tilde{b}_j x + \tilde{c}_j = \frac{\left(Cs_{cell} + \frac{C}{q_{SE}} s_M\right)}{\left(m_{avg} Cs_{chg} - s_A\right)t} = p$$

By using the quadratic formula, we can determine the optimal range:

$$x = \frac{-\tilde{b}_j \pm \sqrt{\tilde{b}_j^2 - 4\tilde{a}_j(\tilde{c}_j - p)}}{2\tilde{a}_j}$$

The solution of interest corresponds to the positive branch of the square root. We can identify the crossover point between range intervals by the value of *p*. For example, the crossover $p_{1,2}$ between intervals 1 and 2 is at 150 miles; hence,

$p_{1,2} = \tilde{a}_1(150)^2 + \tilde{b}_1(150) + \tilde{c}_1 = \tilde{a}_2(150)^2 + \tilde{b}_2(150) + \tilde{c}_2$.

Quantity	Description	Base values	Reference
C	Energy consumption, Wh/mile	250 Wh/mile	(*)
f	Fraction of capacity Q that can be delivered by fast charge	0 0.8	No fast charge USABC 2020 Goal
m_{avg}	Average number of miles driven per day	30 miles/day	Pearre et al. [46]
M	Pack mass, kg		$M = Q / q_{SE} = Cx / q_{SE}$
M_0	Reference pack mass	100 kg†	
N_A	Number of adaptation days per year		See Figure 1 and the Appendix
q_{ED}	Energy density	530 Wh/L 750 Wh/L	(*) USABC 2020 Goal
q_{SE}	Specific energy, Wh/kg	250 Wh/kg 350 Wh/kg	(*) USABC 2020 Goal
Q	Pack energy, kWh		$Q = Cx$
s_A	Adaptation cost	55 $/day	Representative rental car cost in the Unites States
s_{cell}	Cell cost per unit energy, $/Wh	150 $/kWh 100 $/kWh	(*) USABC 2020 Goal
s_{chg}	Electricity cost for charging	0.1 $/kWh	Representative electricity cost
s_M	Cost of added mass, $/kg	10 $/kg	Representative cost for added mass in the United States
S	Total cost, $		Equation 1
S_A	Total cost of adaptation, $		$S_A = N_A\left((1+ f)x\right)ts_A$
S_{chg}	Total cost over the pack life for charging, $		Equation 2
S_M	Total cost of added mass, $		$S_M = \left((Cx / q_{SE}) - M_0\right)s_M$
t	Battery life, years	8 years	Representative warranty on an EV battery
x	EV Range	miles	Independent variable for this work
τ	Charge time, hours	0 0.25 hours	No fast charge USABC 2020 Goal

†100 miles range, 250 Wh/mile, and 250 Wh/kg, yielding $M_0 = 100$ kg.

(*) Similar the that of the 2017 Chevrolet Bolt EV.

Table 1. Nomenclature and base values. Care must be taken to use consistent units in the equations.

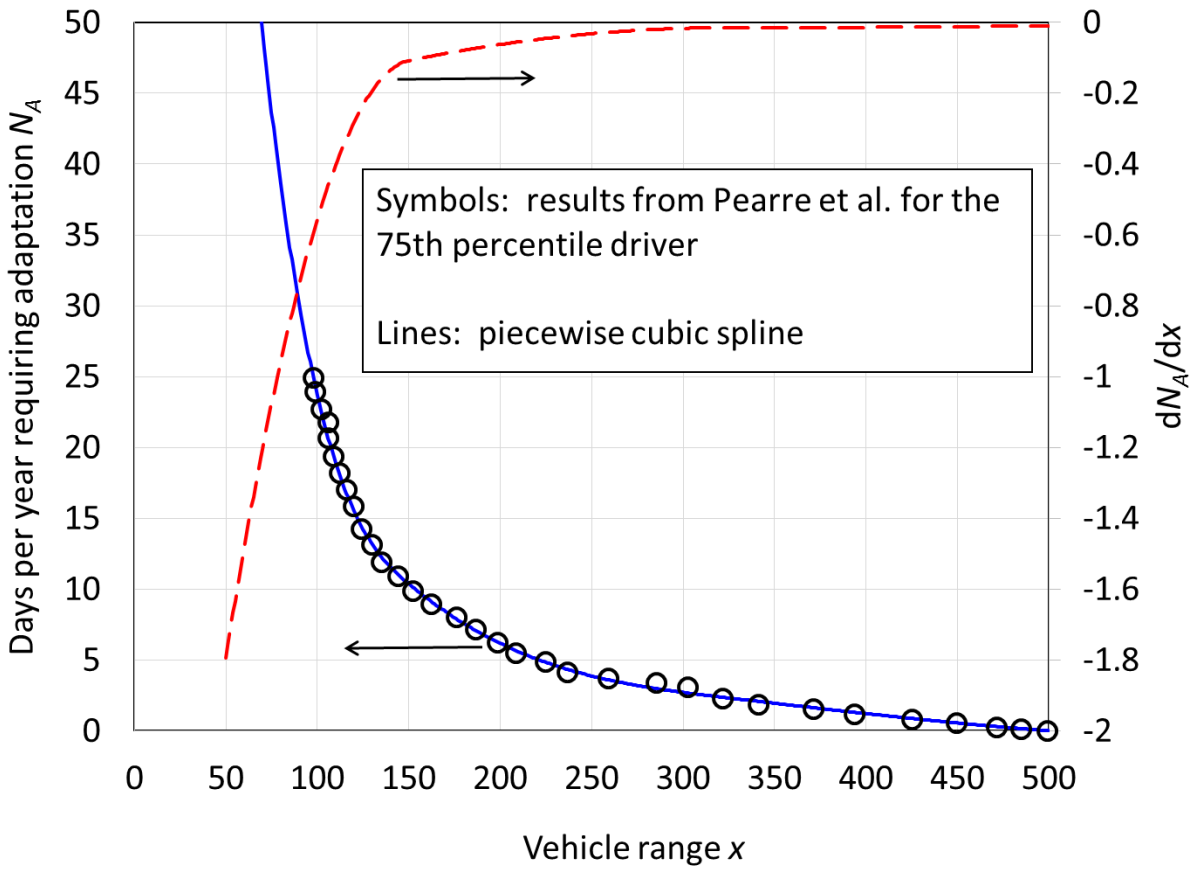

Figure 1. Solid line corresponds to piecewise cubic spline of the Appendix, and the data are from [46].

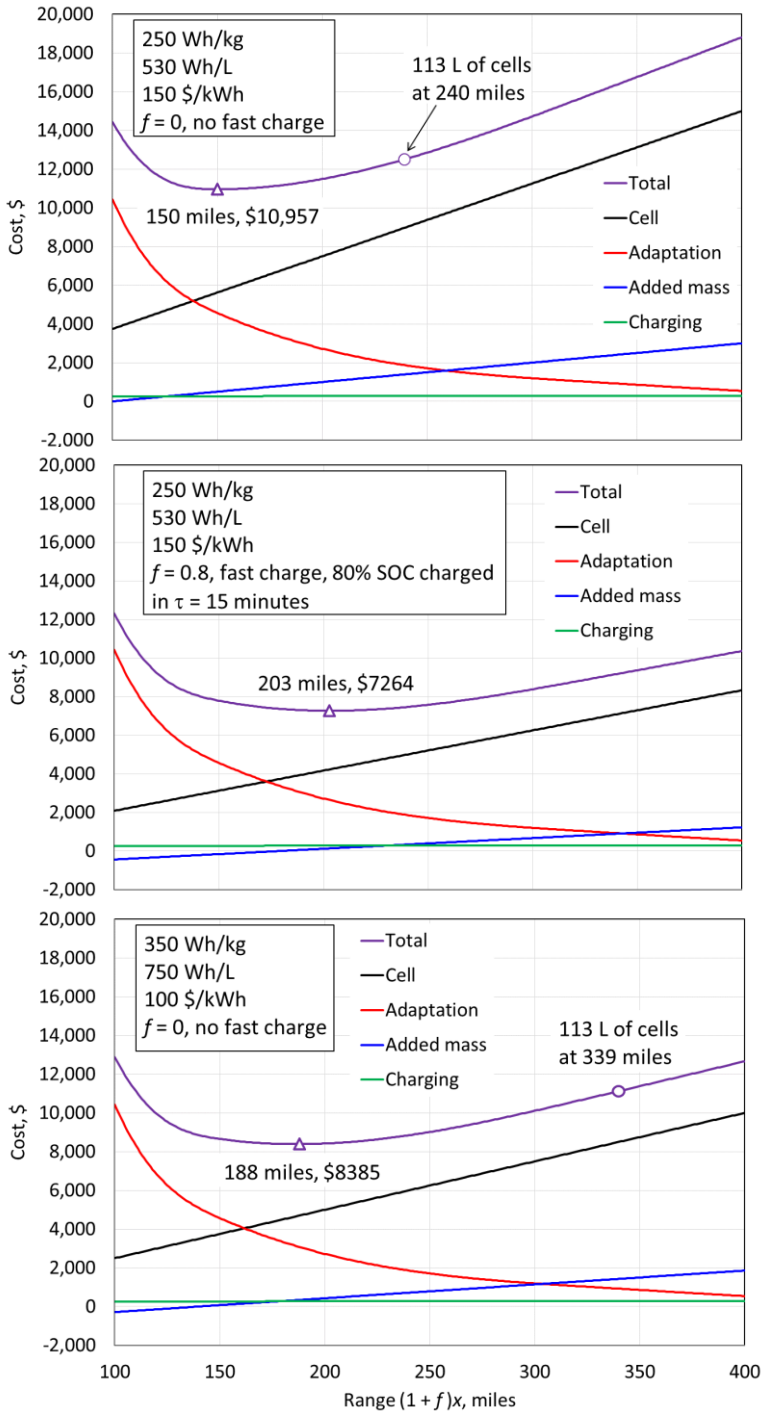

Figure 2. Base scenarios. The conventional lithium ion system (uppermost plot), with fast charge (middle plot), and advanced (high energy density) technology consistent with USABC 2020 goals (and no fast charge) in the lowermost plot.

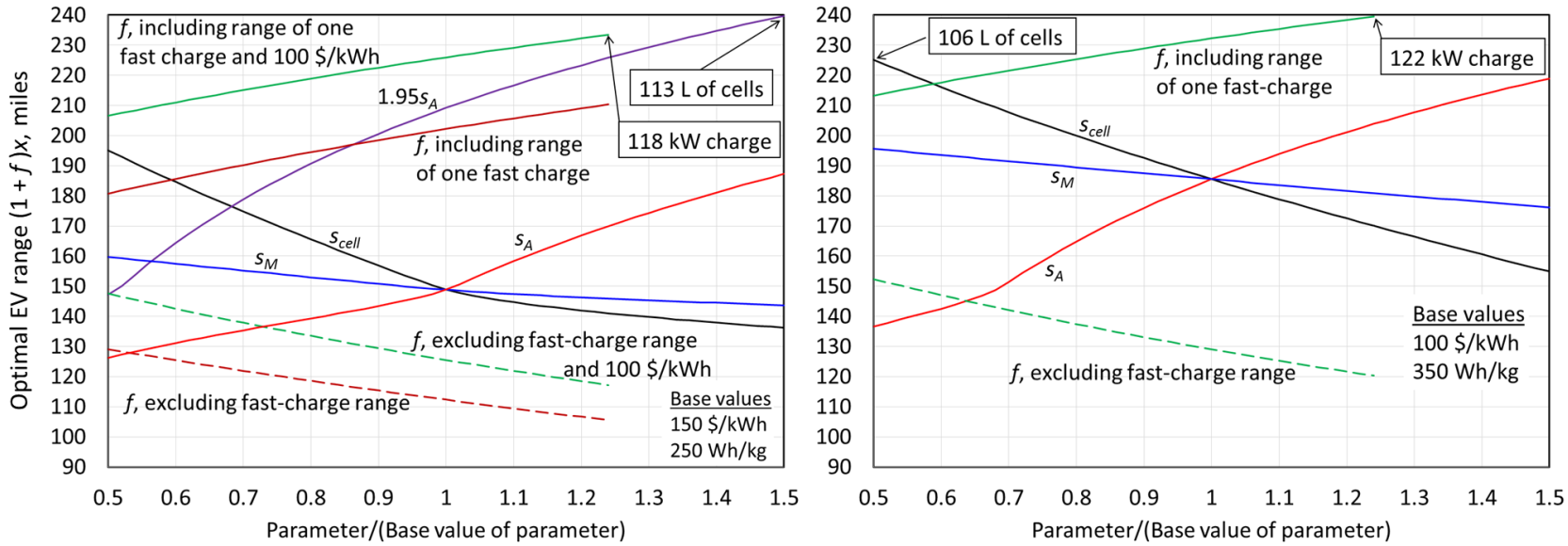

Figure 3. Optimal value of EV range x. The displayed calculations result from solutions to Eq. 5. The ordinate is common to both plots. For the curves labeled s_A, s_{cell}, and s_M, $f = 0$ (no fast charge). Base values for the cell cost ($/kWh) and specific energy (Wh/kg) are provided in each plot. The dashed lines result from subtracting off the range contribution from one fast charge, xf, from the upper curves that reflect the total vehicle range, $(1+f)x$, including one fast charge.

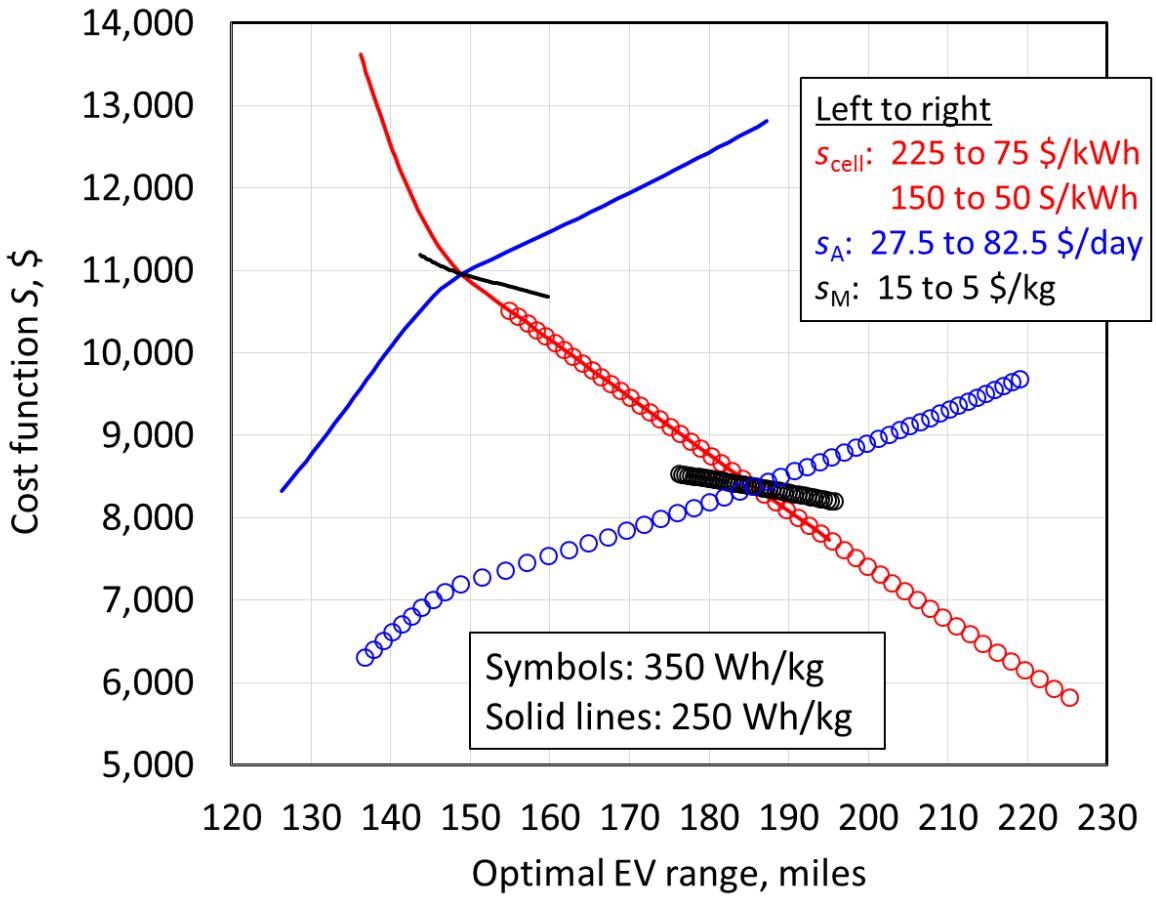

Figure 4. Summation of cost components making up the cost function (Eq. 4) using the optimal value of EV range *x* plotted in Figure 3. The color code in the legend corresponds to the color of the curve and identifies the parameter being varied. The parameter s_{cell} has two ranges: one for the 350 Wh/kg case (symbols, 150 to 50 $/kWh) and one for the 250 Wh/kg case (solid line, 225 to 75 $/kWh). For all cases plotted, $f = 0$ (no fast charge).

References

1. R. Sharma and R. Seefurth, *J. Electrochem. Soc*., *123*(**1976**)1763.
2. J. Graetz, C. C. Ahn, R. Yazami, and B. Fultz, *Electrochemical and Solid-State Letters*, 6(2003)A194.
3. M. N. Obrovac and L. Christensen, *Electrochemical and Solid-State Letters*, *7*(**2004**)A93.
4. S. Ohara, J. Suzuki, K. Sekine, and T. Takamura, *J. Power Sources*, 136(2004)303.
5. M. Uehara, J. Suzuki, K. Tamura, K. Sekine, and T. Takamura, *J. Power Sources*, 146(2005)441.
6. T. Takamura, M. Uehara, J. Suzuki, K. Sekine, K. Tamura, *J. Power Sources*, 158(2006)1401.
7. S. K. Soni, B. W. Sheldon, X. Xiao, and A. Tokranov, *Scripta Materialia*, 64(2011)307.
8. X. Xiao, P. Liu, M. W. Verbrugge, H. Haftbaradaran, and H. Gao, *J. Power Sources*, 196(2011)1409.
9. J. Li, F. Yang, Y-T. Cheng, M. W. Verbrugge, and X. Xiao, *J. Phys. Chem. C*, *116*(**2012**)1472.
10. S. K. Soni, B. W. Sheldon, X. Xiao, M. W. Verbrugge, D. Ahn, H. Haftbaradaran, H. Gao, *J. Electrochem. Soc.*, 159(2012)A38.
11. L. Martin, H. Martinez, M. Ulldemolins, B. Pecquenard, and F. Le Cras, *Solid State Ionics*, 215(2012)36.
12. H. Haftbaradaran, X. Xiao, M. W. Verbrugge, and H. Gao, *J. Power Sources*, *206*(**2012**)357.
13. S. K. Soni, B. W. Sheldon, X. Xiao, A. Bower, and M. W. Verbrugge, *J. Electrochem. Soc.*, 159(2012)A1520.
14. J. Li, X. Xiao, Y-T. Cheng, M. Verbrugge, *J. Phys. Chem. Lett.*, 4(2013)3387.
15. Q. Zhang, X. Xiao, Y-T. Cheng, M. W. Verbrugge, *Appl. Phys. Lett.*, 105(2014)061901.
16. J. Li, X. Xiao, Y-T. Cheng, M. Verbrugge, *J. Phys. Chem. Lett.*, 4(2013)3387.
17. V. A. Sethuraman, V. Srinivasan, and J Newman, *J. Electrochem. Soc*., 160(2013)A394.
18. M. Verbrugge, D. Baker, X. Xiao, Q. Zhang, and Y-T. Cheng, *J. Phys. Chem. C.*, 119(2015)5341.
19. M. Verbrugge, D. Baker, and X. Xiao, *J. Electrochem. Soc.*, 163(2016)A262.
20. E. Markevich, G. Salitra, and D. Aurbach, *J. Electrochem. Soc*., 160(2013)A2407.

21. N. Tamura, M. Fujimoto, M. Kamino, and S. Fujitani, *Electrochim. Acta*, 49(2004)1949.
22. N. Tamura, R. Ohshita, M. Fujimoto, M. Kamino, and S. Fujitani, *J. Electrochem. Soc*., 150(2003)A679.
23. J. Yin, M. Wada, K. Yamamoto, Y. Kitano, S. Tanase, and T. Sakai, *J. Electrochem. Soc*., 153(2006) A472.
24. Y-L. Kim, Y-K. Sun, and S-M. Lee, *Electrochim. Acta*, 53(2008)4500.
25. T. Zhang, H .P. Zhang, L. C. Yang, B. Wang, Y. P. Wu, and T. Takamura, *Electrochim. Acta*, 53(2008)5660.
26. C. C. Nguyen and S-W. Song, *Electrochim. Acta*, 55(2010)3026.
27. K. L. Lee, J. Y. Jung, S. W. Lee, H. S. Moon, and J. W. Park, *J. Power Sources*, 130(2004)241.
28. Q. Zhang, X. Xiao, W. Zhou, Y-T. Cheng, M. W. Verbrugge, *Adv. Energy Mater*., 5(2015)5.
29. Q. Zhang, J. Pan, P. Lu, Z. Liu, M. W. Verbrugge, B. W. Sheldon, Y. Qi, Y-T. Cheng, X. Xiao, *Nano Letters*, 16(2016)2011-2016.
30. T. Chen, Q. Zhang, J. Xu, J. Pan, and Y-T. Cheng, *RSC Adv*., 6(2016)29308.
31. Y. Li1, K. Yan, H-W. Lee, Z. Lu, N. Liu, and Yi Cui, *Nature Energy*, DOI: 10.1038/NENERGY.2015.29.
32. R. Jasinski, "Electrochemistry and Application of Propylene Carbonate," a chapter in *Advances in Electrochemistry and Electrochemical Engineering*, Vol. 8, P. Delahay and C. W. Tobias, Editors, Wiley-Interscience, New York (1971).
33. S. G. Meibuhr, *J. Electrochem. Soc*., 117(1970)56 and 118(1971)1320.
34. R. F. Scarr, *J. Electrochem. Soc*., 117(1970)295.
35. J. Jorné and C. W. Tobias, *J. Electrochem. Soc*., 121(1974)994.
36. E. Peled, *J. Electrochem. Soc*. 126(1979)2047.
37. J. D. Genders, W. M. Hedges, and D, Pletcher, *J. Chem. Faraday Trans*. *1*, 80(1984)3399.
38. R. F. Scarr, "Alkali Metals," a chapter in *Encyclopedia of Electrochemistry of the Elements*, Vol. IX, part B, A. J. Bard, Editor, Marcel Dekker, New York (1986).
39. K. S. Aojuia, J. D. Genders, A. D. Holding, and D. Pletcher, *Electrochim. Acta*, 34(1989)1535.
40. M. W. Verbrugge and B. J. Koch, *J. Electrochem. Soc*., 141(1994)3053.

41. G. Zheng, S. W. Lee, Z. Liang, H-W. Lee, K. Yan, H. Yao, H. Wang, W. Li, S. Chu, and Yi Cui, *Nature Nanotechnology*, 9(2014)618.
42. K. J. Harry, D. T. Hallinan, D. Y. Parkinson, A. A. MacDowell, and N. P. Balsara, *Nature Materials*, 13(2014)69.
43. J. Qian, W. A. Henderson, W. Xu, P. Bhattacharya, M. Engelhard, O. Borodin, and J-G. Zhang, *Nature Communications*, 6(2015)6362, DOI: 10.1038/ncomms7362.
44. K. J. Harry, K. Higa, V. Srinivasan, and N. P. Balsara, *J. Electrochem. Soc.*, 163 (2016) A2216.
45. E. Peled and S. Menkin, *J. Electrochem. Soc.*, 164(2017)A1703.
46. N. S. Pearre, W. Kempton, R. L. Guensler, and V. V. Elango, *Transportation Research Part C*, 19(2011)1171.
47. S. D. Conte and C. de Boor, "Elementary Numerical Analysis. An Algorithmic Approach," third edition, McGraw-Hill, New York, NY, 1980. C. de Boor, "A Practical Guide to Splines," revised edition, Springer, New York, NY, 2001.